On the intrinsically low quantum yields of pyrimidine DNA photodamages; evaluating the reactivity of the corresponding CASPT2 MECPs

Angelo Giussani,[1,†,*] Graham A. Worth[1]

[1] Department of Chemistry, University College London, 20 Gordon Street,
London WC1H 0AJ, UK.
[†] Current address: Instituto de Ciencia Molecular, Universidad de Valencia, Catedrático José Beltrán 2, 46980 Paterna, Spain.
* E-mail: angelo.giussani@uv.es

The low quantum yield of photoformation of cyclobutane pyrimidine dimers and pyrimidine-pyrimidone (6−4) adducts in DNA bases is usually associated with the presence of more favorable non-reactive decay paths and with the unlikeliness of exciting the system in a favorable conformation. Here we prove that the ability of the reactive conical intersection to bring the system either back to the absorbing conformation or to the photoproduct must be considered as a fundamental factor in the low quantum yields of the mentioned photodamages. In support of the proposed model, the one order of magnitude difference in the quantum yield of formation of the cyclobutane thymine dimer with respect to the thymine-thymine (6-4) adduct is rationalized here by comparing the reactive ability of the seam of intersections leading respectively to the cyclobutane thymine dimer and the oxetane precursor of the thymine-thymine (6-4) adduct at the CASPT2 level of theory.

Cyclobutane pyrimidine dimers (CPDs) and pyrimidine-pyrimidone (6−4) adducts (PPAs) are UV-induced DNA photodamages with mutagenic and carcinogenic properties.[1] CPDs are the result of a [2+2] photocycloaddition between the carbon-carbon double bonds of two consecutive pyrimidine nucleobases belonging to the same DNA strand.[2-6] The reaction can proceed in both the singlet and triplet manifolds (in fact CPDs have been detected both after direct UV absorption and in the presence of photosensitizers)[7,8] and under UVA and UVB irradiation.[9] The process is ultrafast, as proven by the seminal work of Zinth, Kohler and co-workers for the particular case of two reactive thymine nucleobases forming the cyclobutane thymine dimer (Figure 1a) in the all-thymine oligodeoxynucleotide $(dT)_{18}$ system, where the timescale of the reaction was recorded to be around 1 ps.[10]

PPAs are the results of the reaction between a carbon-carbon double bond and either a carbonyl or an amide group of two consecutive pyrimidine nucleobases belonging to the same DNA strand (Figure 1b). It is normally accepted that the reaction takes place via oxetane or azedine intermediates, their formation being the actual photoactivated part of the global process, followed by thermal ring opening toward the final PPA product.[2,6,11–13] In the case of two reactive thymine nucleobases, the first photoactivated part of the mechanism leading to an oxetane structure is a so called Paternò-Büchi reaction (Figure 1b).[14] In contrast to CPDs, PPAs are not formed under UVA radiation.[9] The mechanism has been proposed to occur along the singlet manifold,[6,15] even if a possible involvement of triplet states (which indeed have a recognized importance in the general mechanism of the Paternò-Büchi reaction)[16] has been suggested and never completely ruled out.[12] The timescale for the formation of the oxetane intermediate has never been experimentally recorded, although it is assumed to proceed in the ultrafast regime.[17]

The quantum yield of formation (Φ_f) of both CPDs and PPAs has been proven to depend on different factors, among which one of the most important is the nature of the two involved pyrimidine nucleobases.[18] In the case of thymine-thymine (6-4) adduct, the quantum yield in thymine strands has been shown to be proportional to the energy of the excitation wavelength, while such a dependence was not detected for the cyclobutane thymine dimer.[6] The experimentally

observed Φ_f for DNA strands are however very low, ranging from 10^{-3} to 10^{-5}, depending on the type of photoproducts and on the specific conditions.[19] This fortunate - at least for a human health perspective - condition is normally rationalized by the presence of competitive non-reactive decay paths.[20,21] The relative importance of environmental effects and the intrinsic photophysical properties of the thymine molecules is still to be determined.

Zinth, Kohler and co-workers, introduced the concept of initial reactive conformation[10]: "*The low yields for all-thymine oligomers thus reveal that only a few percent of the TT doublets are favorably positioned for reaction at the time of excitation*". It is the conformation of the system at the time of light irradiation which mainly determines if the photoresponse will either lead to the photoproduct or not.[22] Following this line of thought, theoretical models have emerged in which CPDs and PPAs Φ_f of different systems were computed through the estimation of the percentage of thermally accessible ground state conformations characterized by one or more particular geometrical features, assumed to be key for the pro-reactivity of the system.[23,24] In turn these geometrical features were determined evaluating the subsequent evolution of the excited states, mostly focusing on the ability to reach a conical intersection region connected with the photoproduct.[15] As far as we are concerned, little effort has been devoted to the description of the subsequent evolution after ground state repopulation at the reactive seam of intersection, with only one paper, presented by one of us, showing that for the thymine-thymine (6−4) photolesion the conical intersection (CI) leading to the photoproduct is not the first encountered point of the CI seam.[13]
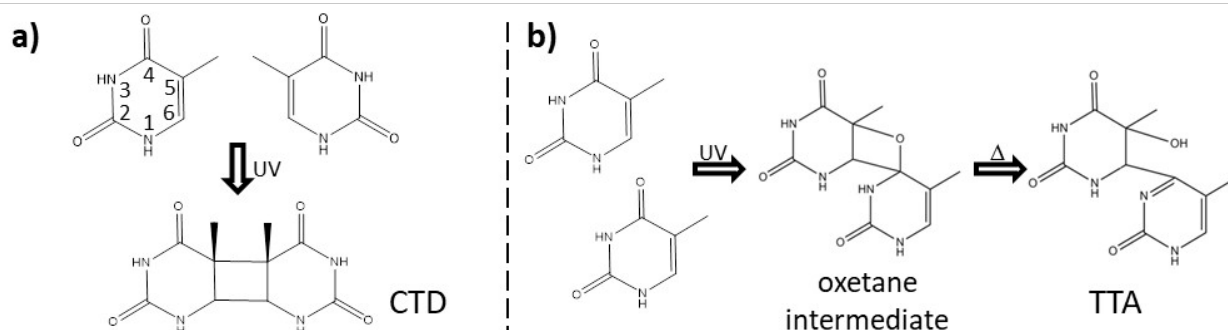
Figure 1. a) Scheme of the reaction leading to the cyclobutane thymine dimer (CTD); b) Scheme of the reaction leading to the thymine-thymine (6-4) adduct (TTA). Atom labelling is also reported.

In the present contribution we have evaluated the ability of what are now recognized as the CI regions responsible respectively for the formation of the cyclobutane thymine dimer (CTD) and the thymine-thymine (6-4) adduct (TTA) to actually bring the system to the corresponding photoproduct.[5,12] This was done by performing ab initio CASPT2//CASSCF and CASPT2//CASPT2[25] computations as implemented in the OpenMolcas[26] code on a model system composed of two isolated thymine molecules. Our aim was to evaluate how the efficiency of such CI regions to lead to photoformation impacts on the Φ_f of the two photoreactions by an evaluation of their topology.

CIs are not isolated structures but form a locus of points. It is consequently not possible to compare two CI-mediated photoreactions by comparing the corresponding CI in the way ground-state reactions are compared by examining the transitions states. One can compare the corresponding minimum energy crossing points (MECPs, i.e. a minimum in the CI seam), but it must be kept in mind that a process could occur without the need to reach the MECP, since other CI points could be more accessible.[27] The efficiency of a CI to mediate population transfer and to promote, or hinder, reactivity can be evaluated by characterizing its topology, although only dynamics simulations are capable of providing a quantitative analysis. CIs can be classified as either peaked or sloped.[28,29]. Peaked CI are more efficient than sloped CI in promoting population transfer from the upper to the

lower state.[30] CIs can also be subdivided into two further categories: single-path and bifurcating.[31] Single-path CIs have only one preferred relaxation direction on the lower potential energy hypersurface (PEH), while for bifurcating CIs, there are two such directions. Consequently single-path CIs will preferably give rise to a single photoproduct, while two different photoproducts can results from bifurcating CIs.

Starting with the analysis of the TTA photoformation, a CASPT2(16,12) MECP optimization between the S1 and S0 states was performed, which resulted in the characterization of the MECP structure hereafter denoted as $(S1/S0)_{mecp-TTA}$ (Figure 2). At this structure the states are separated by 0.01 eV at the CASPT2(16,12) level. The computation, as all others here presented, was performed using a basis set of atomic natural orbital (ANO)[32] of S-type contracted to C,N,O[3s,2p,1d]/H[2s1p] and with an active space (16 active electrons distributed in 12 active orbitals) which includes the most relevant π orbitals. Due to the lack of analytical CASPT2 gradients, all CASPT2 optimizations are numerical. The latter point is a known source of numerical errors.[33] For this reason, and for the associated prohibitively high computational cost, the nature of the obtained CASPT2 critical points was not verified by computing numerical CASPT2 frequencies. As an estimation, the corresponding CASSCF(16,12) frequencies were calculated. At this level of theory an imaginary frequency of 231 cm^{-1} was computed at the $(S1/S0)_{mecp-TTA}$ structure, consequently partially supporting the MECP character of the latter structure.

In order to evaluate the further evolution of the system from the $(S1/S0)_{mecp-TTA}$ point, CASSCF(16,12) minimum energy paths (MEPs) computations were performed. Being a CI, at the $(S1/S0)_{mecp-TTA}$ geometry the distinction between S0 and S1 is ill-defined. For that reason, a MEP computation was performed following the nature of each of the two crossing states,[34] each of which, depending of the direction along which the system evolves, could energetically become the S0 state. The MEP following the upper state (i.e. the one for which a single imaginary frequency was computed) evolves towards the formation of the oxetane intermediate, while the other MEP decays back to two separate thymine molecules. The result points out that $(S1/S0)_{mecp-TTA}$ can indeed mediate the photoreaction, if the system evolves following the nature of the initially upper state.

To gain further knowledge of the process, the topology of the $(S1/S0)_{mecp-TTA}$ CI has been determined, again for computational reasons at the CASSCF level, as implemented in the OpenMolcas code.[31] This approximation is partially justified here by the near degeneracy displayed also at this level of theory (0.10 eV energy difference). The analysis determined that the $(S1/S0)_{mecp-TTA}$ CI is peaked and bifurcating. The bifurcating character is in agreement with the computed MEPs (one leading to photoreaction, the other not) while the peaked character tells us that the CI has a propensity to transfer population from the upper to the lower state.

A second CASPT2(16,12) S0/S1 MECP optimization was performed to explore the CI region from a different starting point. For the new structure obtained, hereafter $(S1/S0)_{mecp-TTA-2}$ (Figure 2), a similar analysis to the one described above for $(S1/S0)_{mecp-TTA}$ was performed. Geometrically the two MECP structures are very similar, being energetically separated by only 0.02 eV. At the $(S1/S0)_{mecp-TTA-2}$ the S0 and S1 states are completely degenerate at the CASPT2(16,12) level (while 0.30 eV apart at CASSCF level), and two imaginary CASSCF frequencies of 133 and 71 cm^{-1} were obtained. Despite these similarities, two fundamental differences differenciate the MECPs. First, from $(S1/S0)_{mecp-TTA-2}$ both MEP, each of which follow the nature of either the upper or the lower state, evolve in a non-reactive way towards the two separated nucleobases. Second, the $(S1/S0)_{mecp-TTA-2}$ CI is still peaked, but this time is single-pathed, in agreement with the common evolution recorded along the two MEPs. It is significant to note that at the non-reactive $(S1/S0)_{mecp-TTA-2}$ the CO bond being formed is shorter than at the reactive $(S1/S0)_{mecp-TTA}$ (1.754 vs 1.784 Å). However, the reactive $(S1/S0)_{mecp-TTA}$ displays a more puckered C4 atom (forming the new CC bond in the

oxetane structure) than $(S1/S0)_{mecp-TTA-2}$ (Figure 2). This latter feature was already reported to strongly influence the pro-reactivity of the CI.[13]

From the analysis presented, we can therefore conclude that the CI responsible for the photoformation of the TTA photodamage would preferably bring the system back to two separated thymines. This in turn should be an important factor in the low Φ_f reported for this photoproduct (around 10^{-4}), which is indeed one of the least formed dipyrimidine photodamages.[19]
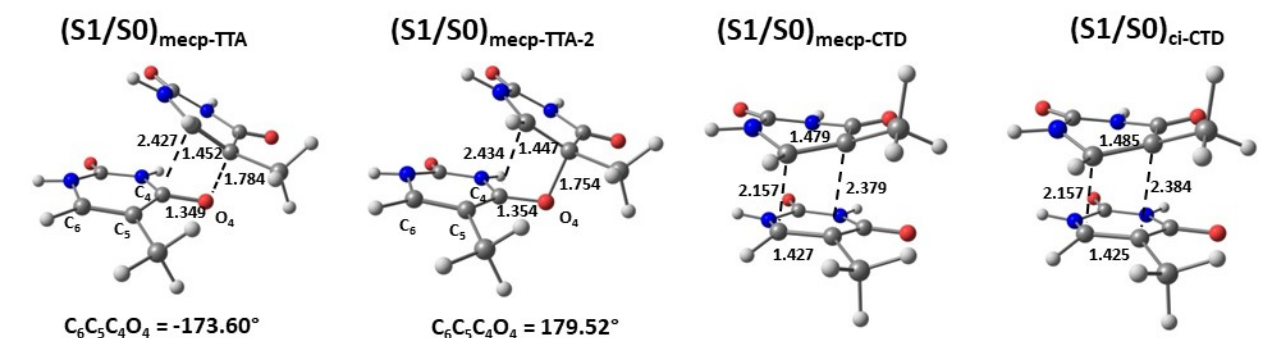
Figure 2. Geometries of the MECPs and CIs discussed in the text. Selected bond lengths (in Å) and angles (in deg) are also reported.

Let us now turn to the CTD photoreaction. An analogous exploration to the one described for TTA was undertaken. This time only one CASPT2(16,12) MECP was obtained, hereafter $(S1/S0)_{mecp-CTD}$ (Figure 2). In the latter structure the S0 and S1 states are completely degenerate at the CASPT2(16,12) level (0.54 eV at CASSCF level), and no imaginary CASSCF frequencies were computed. The MECP CASSCF topology is peaked and bifurcating. The bifurcating character is supported by the computed MEP profiles: the upper state evolves towards CTD formation, the lower state decays back to the separated nucleobases.

To evaluate if a non-reactive region of the CI seam also exists for the CTD case analogous to that found for the TTA photoreaction, a series of geometries were built distorting the $(S1/S0)_{mecp-CTD}$ CI along the direction of the non-zero CASSCF gradient of the S1 state, projecting onto the seam space so as to keep the degeneracy. The branching space was computed at the CASSCF level.[31] For the so defined structures $((S1/S0)_{ci-CTD-0.5}, (S1/S0)_{ci-CTD-0.6}$, etc), the S0-S1 degeneracy has been calculated at the CASPT2 level, the potential evolution of the system has been evaluated by computing MEPs, and the topology of each CI has been characterized at the CASSCF level (Table S1). The first structure for which both CASSCF MEPs describe a non-reactive path is $(S1/S0)_{ci-CTD-0.7}$, hereafter $(S1/S0)_{ci-CTD}$ (Figure 2), which is placed 0.71 eV above the $(S1/S0)_{mecp-CTD}$ geometry. The main geometrical deformation with respect to the $(S1/S0)_{mecp-CTD}$ point is the elongation of the carbonyl groups (Figure S3). At $(S1/S0)_{ci-CTD}$ the S0 and S1 states are separated by 0.05 eV at the CASPT2 level (0.41 eV at CASSCF level) and the CI can be topologically classified as peaked and bifurcating. The latter feature is in discord with the two coincident MEP evolutions; however, the parameter that determines the bifurcating or single-path topology shows that this structure is not very far from a single-path topology,[35] and in fact along this direction a nearby single-path CI point $((S1/S0)_{ci-CTD-0.9})$ has been located (Table S1).

The nature of the S1 state at the CI points analyzed here has also been characterized for both systems. As shown in Figure S1, at both the characterized MECPs related to the TTA photoproduct the S1 state mostly describes a charge transfer state from the thymine molecule bearing the reactive carbon-carbon double bond toward the thymine molecule where the reactive carbonyl group is placed. In contrast, as presented in Figure S2, at both the $(S1/S0)_{ci-CTD}$ and $(S1/S0)_{mecp-CTD}$ structures the S1 state is delocalized over the two reactive carbon-carbon double bonds, and

consequently over the two nucleobases. These assignments of the S1 state are in agreement with previous works.[5,6,12,13,15]

It is now instructive to compare the results obtained regarding the TTA and CTD photoformation. In both cases a CASPT2(16,12) MECP belonging to the seam of intersection responsible for the corresponding photoreaction has been characterized. Both MECPs, the $(S1/S0)_{mecp-TTA}$ and $(S1/S0)_{mecp-CTD}$ structures, respectively, are peaked and bifurcating CI, and in both cases the computed MEP following the nature of the upper state evolves toward the photoproduct while the corresponding MEP following the nature of the lower state decays back to the two separated nucleobases. A second MECP, $(S1/S0)_{mecp-TTA-2}$, associated with the TTA photoreaction and placed only 0.02 eV above the $(S1/S0)_{mecp-TTA}$ MECP has been localized. Such a MECP is peaked but single-pathed, and in fact both MEPs evolve in a non-reactive fashion. A CI whose evolution is only non-reactive has been also characterized for CTD, the $(S1/S0)_{ci-CTD}$ geometry, but in this case it is placed 0.71 eV above the $(S1/S0)_{mecp-CTD}$ MECP and it is not a MECP.

These analogies and differences prompt us to the following conclusions. First, although connected to the photoproduct, both seams of intersection have a non-negligible tendency towards non-reactivity. This factor should be taken into consideration when evaluating the efficiency of the global photoreactions, and is a possible intrinsic factor determining the low Φ_f of such photodamages. Second, the TTA photoreaction is intrinsically less efficient than the CTD photoformation, since a completely non-reactive MECP for TTA has been characterized to be practically degenerate with the lowest MECP, while for CTD the non-reactive region is placed 0.71 eV above the MECP. In agreement with such a model is the fact that the Φ_f of TTA is an order of magnitude lower than the Φ_f of CTD.[18,19]
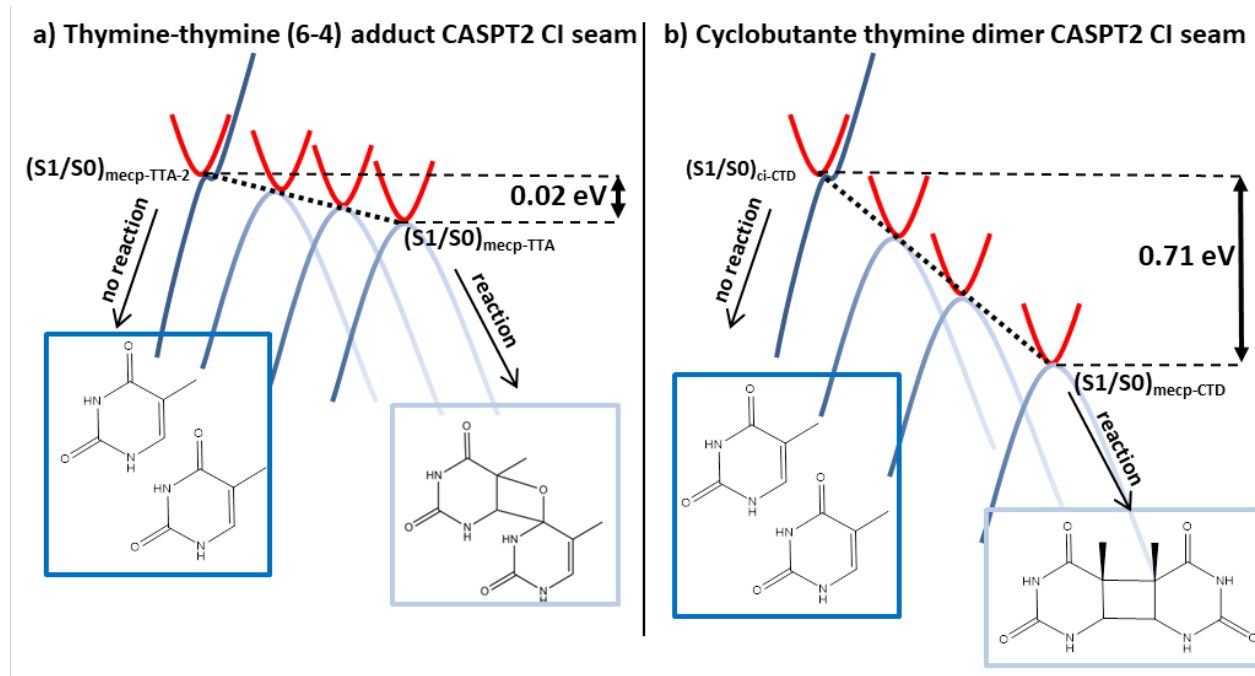
Figure 3. a) Schematic representation on the CASPT2 CI seam leading to the thymine-thymine (6-4) adduct; b) Schematic representation on the CASPT2 CI seam leading to the cyclobutane thymine dimer.

Summarizing, a model based on CASPT2 characterizations of the seam of intersections has been presented. The model, pictorially represented in Figure 3, provides an intrinsic justification of the low quantum yield of formation of the cyclobutane thymine dimer and the thymine-thymine (6-4) adduct photoproducts, and qualitatively explains the one order of magnitude difference in their

quantum yield of formation. It must be noted that the experimental values are actually referring to the global processes (i.e. the formation of CTD and TTA), while the present model is comparing the formation of CTD with the formation of the oxetane intermediate, normally assumed to be the photoproduct which subsequently undergoes a thermally activated reaction to the final TTA molecule. The efficiency of this thermal reaction would consequently influence the detected global quantum yields. However, the results obtained here, although not dealing with the global (photoactivated plus thermal) process toward TTA production, represent an intrinsic molecular reason for the lower efficiency of the mechanism of formation of TTA with respect to CPD.

In the present contribution the focus is on the evolution that the system can experience after the decay from the seam of the reactive CI, and not on how the system can reach these regions after light absorption. The latter question was the subject of previous works,[6,13,15] among which the paper of Conti et al. in which, working on a B-DNA oligonucleotide duplex and a $(dA)2 \cdot (dT)2$ dimer, a series of geometrical parameters not only related to the distance of the reactive atoms was shown to strongly influence the propensity of an initial structure to reach the reactive CI.[15] In agreement with the previous paper of Markovitsi, Improta and coworkers, both barrierless and non-barrierless decay paths were characterized for reaching the CIs related to the cyclobutane thymine dimer and thymine-thymine (6-4) adduct photoproduct, respectively. Such a result was associated with the increase in the thymine-thymine (6-4) adduct Φ_f with the excitation energy (being actually zero under UVA radiation), a trend instead not observed for the cyclobutane thymine dimer Φ_f (which is formed under both UVA and UVB irradiation).[6] The thymine-thymine (6-4) adduct Φ_f dependence with the excitation wavelength was in another paper instead associated with the presence of an energy barrier situated in the seam of intersection and not along the path leading to it.[13] Here, although the reported trend in the Φ_f has not been addressed, the non-reactive MECP point described here for the TTA reaction (i.e. geometry $(S1/S0)_{mecp-TTA-2}$) demonstrates the need to reach energetically higher CI points to have an efficient reaction, which is in partial agreement with reference 13.

The limitations of the present treatment should however been kept in mind. First, the work aimed at depicting the intrinsic properties of the photoprocess; a predictable significant effect of a surrounding DNA environment is not taken into consideration here. Second, the analysis of the CIs topology is based on a linear model, consequently it is only valid in the vicinity of the CI. Third, the direction from the $(S1/S0)_{mecp-CTD}$ structure here analyzed (projection of the S1 CASSCF gradient on the CASSCF intersection space) in order to explore the CI seam in search for a completely non-reactive CI point (indeed found in the $(S1/S0)_{ci-CTD}$ structure) does not guarantee the absence of other completely non-reactive CI points lower in energy, present along a different direction. A lower completely non-reactive CI point has however not been found here. Moreover, along the analyzed direction, it is possible to observe how the topology of the CI is gradually changing from bifurcating to single-pathed (Table S1). Despite these limitations, the obtained picture, which is in qualitative agreement with the experimental Φ_f, speaks in favor of the reliability of the analysis.

(1)   Ichihashi, M.; Ueda, M.; Budiyanto, a.; Bito, T.; Oka, M.; Fukunaga, M.; Tsuru, K.; Horikawa, T. UV-Induced Skin Damage. *Toxicology* **2003**, *189* (1–2), 21–39.

(2)   Migani, A.; Blancafort, L. Modeling Thymine Photodimerizations in DNA: Mechanism and Correlation Diagrams. *J. Am. Chem. Soc.* **2007**, *129*, 14540–14541.

(3)   Boggio-pasqua, M.; Groenhof, G.; Scha, L. V; Robb, M. A. Ultrafast Deactivation Channel for Thymine Dimerization. *J. Am. Chem. Soc.* **2007**, *129*, 10996–10997.

(4)   Roca-Sanjuán, D.; Olaso-González, G.; González-Ramírez, I.; Serrano-Andrés, L.; Merchán, M. Molecular Basis of DNA Photodimerization: Intrinsic Production of Cyclobutane Cytosine Dimers. *J. Am. Chem. Soc.* **2008**, *130* (32), 10768–10779.

(5)   Serrano-Pérez, J. J.; González-Ramírez, I.; Coto, P. B.; Merchán, M.; Serrano-Andrés, L. Theoretical Insight into the Intrinsic Ultrafast Formation of Cyclobutane Pyrimidine Dimers in UV-Irradiated DNA: Thymine versus Cytosine. *J. Phys. Chem. B* **2008**, *112* (45), 14096–14098.

(6)   Banyasz, A.; Douki, T.; Improta, R.; Gustavsson, T.; Onidas, D.; Vayá, I.; Perron, M.; Markovitsi, D. Electronic Excited States Responsible for Dimer Formation upon UV Absorption Directly by Thymine Strands: Joint Experimental and Theoretical Study. *J. Am. Chem. Soc.* **2012**, *134* (36), 14834–14845.

(7)   Cadet, J.; Mouret, S.; Ravanat, J.-L.; Douki, T. Photoinduced Damage to Cellular DNA: Direct and Photosensitized Reactions. *Photochem. Photobiol.* **2012**, *88* (5), 1048–1065.

(8)   Climent, T.; González-Ramírez, I.; González-Luque, R.; Merchán, M.; Serrano-Andrés, L. Cyclobutane Pyrimidine Photodimerization of DNA/RNA Nucleobases in the Triplet State. *J. Phys. Chem. Lett.* **2010**, *1* (14), 2072–2076.

(9)   Baudouin, C.; Charveron, M.; Favier, A.; Cadet, J.; Douki, T. Cyclobutane Pyrimidine Dimers Are Predominant DNA Lesions in Whole Human Skin Exposed to UVA Radiation. **2006**, *103* (37), 13765–13770.

(10)   Schreier, W. J.; Schrader, T. E.; Koller, F. O.; Gilch, P.; Crespo-hernández, C. E.; Swaminathan, V. N.; Carell, T.; Zinth, W.; Kohler, B. Thymine Dimerization in DNA Is an Ultrafast Photoreaction. **2007**, *315*, 625–629.

(11)   Yang, Z. B.; Eriksson, L. A.; Zhang, R. B. A Theoretical Rationale for Why Azetidine Has a Faster Rate of Formation than Oxetane in TC(6-4) Photoproducts. *J. Phys. Chem. B* **2011**, *115* (31), 9681–9686.

(12)   Giussani, A.; Serrano-Andrés, L.; Merchán, M.; Roca-Sanjuán, D.; Garavelli, M. Photoinduced Formation Mechanism of the Thymine-Thymine (6-4) Adduct. *J. Phys. Chem. B* **2013**, *117* (7), 1999–2004.

(13)   Giussani, A.; Conti, I.; Nenov, A.; Garavelli, M. Photoinduced Formation Mechanism of the Thymine-Thymine (6-4) Adduct in DNA; A QM(CASPT2//CASSCF):MM(AMBER) Study. *Faraday Discuss.* **2018**, *207*, 375–387.

(14)   Paterno, E.; Chiefi, G. *Gazz. Chim. Ital.* **1909**, *39*, 431.

(15)   Conti, I.; Martínez-Fernández, L.; Esposito, L.; Hofinger, S.; Nenov, A.; Garavelli, M.; Improta, R. Multiple Electronic and Structural Factors Control Cyclobutane Pyrimidine

Dimer and 6–4 Thymine–Thymine Photodimerization in a DNA Duplex. *Chem. - A Eur. J.* **2017**, *23* (60), 15177–15188.

(16) Brogaard, R. Y.; Schalk, O.; Boguslavskiy, A. E.; Enright, G. D.; Hopf, H.; Raev, V.; Tarcoveanu, E.; Sølling, T. I.; Stolow, A. The Paternò-Büchi Reaction: Importance of Triplet States in the Excited-State Reaction Pathway. *Phys. Chem. Chem. Phys.* **2012**, *14* (24), 8572–8580.

(17) Marguet, S.; Markovitsi, D. Time-Resolved Study of Thymine Dimer Formation. *J. Am. Chem. Soc.* **2005**, *127* (16), 5780–5781.

(18) Douki, T.; Cadet, J. Individual Determination of the Yield of the Main UV-Induced Dimeric Pyrimidine Photoproducts in DNA Suggests a High Mutagenicity of CC Photolesions. *Biochemistry* **2001**, *40*, 2495–2501.

(19) Douki, T. The Variety of UV-Induced Pyrimidine Dimeric Photoproducts in DNA as Shown by Chromatographic Quantification Methods. *Photochem. Photobiol. Sci.* **2013**, *12* (8), 1286–1302.

(20) Giussani, A.; Segarra-Martí, J.; Roca-Sanjuán, D.; Merchán, M. Excitation of Nucleobases from a Computational Perspective I: Reaction Paths. *Top. Curr. Chem.* **2013**, *355*, 57.

(21) Francés-Monerris, A.; Gattuso, H.; Roca-Sanjuán, D.; Tuñón, I.; Marazzi, M.; Dumont, E.; Monari, A. Dynamics of the Excited-State Hydrogen Transfer in a (DG)·(DC) Homopolymer: Intrinsic Photostability of DNA. *Chem. Sci.* **2018**, *9* (41), 7902–7911.

(22) Schreier, W. J.; Kubon, J.; Regner, N.; Haiser, K.; Schrader, T. E.; Zinth, W.; Clivio, P.; Gilch, P. Thymine Dimerization in DNA Model Systems: Cyclobutane Photolesion Is Predominantly Formed via the Singlet Channel. *J. Am. Chem. Soc.* **2009**, 131, 5038–5039.

(23) Hariharan, M.; Mccullagh, M.; Schatz, G. C.; Lewis, F. D. Conformational Control of Thymine Photodimerization in Single-Strand and Duplex DNA Containing Locked Nucleic Acid TT Steps. *J. Am. Chem. Soc.* **2010**, *132*, 12856–12858.

(24) Hariharan, M.; Siegmund, K.; Saurel, C.; McCullagh, M.; Schatz, G. C.; Lewis, F. D. Thymine Photodimer Formation in DNA Hairpins. Unusual Conformations Favor (6 - 4) vs. (2 + 2) Adducts. *Photochem. Photobiol. Sci.* **2014**, *13* (2), 266–271.

(25) Andemson, K.; Malmqvist, P.; Roos, B.; Sadlej, A. J.; Wolinskit, K. Second-Order Perturbation Theory with a CASSCF Reference Function. **1990**, No. 7, 5483–5488.

(26) Fernández Galván, I.; Vacher, M.; Alavi, A.; Angeli, C.; Aquilante, F.; Autschbach, J.; Bao, J. J.; Bokarev, S. I.; Bogdanov, N. A.; Carlson, R. K.; et al. OpenMolcas: From Source Code to Insight. *J. Chem. Theory Comput.* **2019**, *15*, 5925–5964.

(27) Giussani, A.; Merchán, M.; Gobbo, J. P.; Borin, A. C. Relaxation Mechanisms of 5-Azacytosine. *J. Chem. Theory Comput.* **2014**, *10*, 3915.

(28) Matsika, S.; Krause, P. Nonadiabatic Events and Conical Intersections. *Annu. Rev. Phys. Chem.* **2011**, *62* (1), 621–643.

(29)   Atchity, G. J.; Xantheas, S. S.; Ruedenberg, K. Potential Energy Surfaces near Intersections. *J. Chem. Phys.* **1991**, *95* (3), 1862.

(30)   Ben-Nun, M.; Molnar, F.; Schulten, K.; Martínez, T. J. The Role of Intersection Topography in Bond Selectivity of Cis-Trans Photoisomerization. *Proc. Natl. Acad. Sci. U. S. A.* **2002**, *99* (4), 1769–1773.

(31)   Galván, I. F.; Delcey, M. G.; Pedersen, T. B.; Aquilante, F.; Lindh, R. Analytical State-Average Complete-Active-Space Self-Consistent Field Nonadiabatic Coupling Vectors: Implementation with Density-Fitted Two-Electron Integrals and Application to Conical Intersections. *J. Chem. Theory Comput.* **2016**, *12* (8), 3636–3653.

(32)   Pierloot, K.; Dumez, B.; Widmark, P.-O.; Roos, B. O. Density Matrix Averaged Atomic Natural Orbital (ANO) Basis Sets for Correlated Molecular Wave Functions. *Theor. Chim. Acta* **1995**, *90*, 87.

(33)   Giussani, A.; Worth, G. A. Similar Chemical Structures, Dissimilar Triplet Quantum Yields: A CASPT2 Model Rationalizing the Trend of Triplet Quantum Yields in Nitroaromatic Systems. *Phys. Chem. Chem. Phys.* **2019**, *21* (20), 10514–10522.

(34)   With OpenMolcas (See Reference 26) It Is Possible to Follow the Nature of a Particular State along an Optimization through the Evaluation in Each Step of the State Overlaps with the RASSI Module.

(35)   If B>1 the CI Is Single-Path, If B<1 the CI Is Bifurcating (See Reference 31). Here It Is Equal to 0.97.